

# The 1024 channel digital correlator receiver of the Gauribidanur radioheliograph

R. Ramesh · M. S. Sundara Rajan · Ch. V. Sastry

Received: 29 December 2005 / Accepted: 20 July 2006  
© Springer Science + Business Media B.V. 2007

**Abstract** A low frequency (40–150 MHz) radioheliograph for observations of the solar corona is in operation for the last few years at the Gauribidanur radio observatory, about 100 km north of Bangalore. The array has 32 antenna groups and a 1-bit digital correlator system consisting of 1024 channels is used as the back-end receiver. This paper describes the latter and results of the associated system tests.

**Keywords** Aperture synthesis · Digital correlator · Interferometry · Radio telescopes

## 1. Introduction

The Gauribidanur radioheliograph (GRH) is a T-shaped interferometer array for observations of the solar corona and it operates in the 40–150 MHz range. The arms of the ‘T’ are oriented in the East-West and South direction. The basic receiving element used is a Log Periodic Dipole (LPD, [8]). There are 192 LPDs in the array and they are arranged as 32 groups (refer [14, 15] for details about the GRH).

## 2. The 1024 channel digital correlator

In order to carry out multiplications between all the 32 antenna groups in the GRH, a 1-bit digital correlator consisting of 1024 channels is used (refer [3, 5, 21, 23] for details on 1-bit correlation technique). To beginwith, the cosine and sine IF signal ( $f_c = 10.7$  MHz and  $\Delta f = 1$  MHz) from the analog receiver are quantised to two levels (+1 or 0) using a zero crossing detector. The basic element used here is the high speed comparator (AD 790). Its

---

R. Ramesh (✉) · M. S. Sundara Rajan  
Indian Institute of Astrophysics, Bangalore 560 034  
e-mail: ramesh@iiap.res.in

Ch. V. Sastry  
‘MEENAKSHI’, No. 3, 2nd Cross, 1st Block, Koramangala, Bangalore 560 034

output is either a TTL ‘high’ or ‘low’ depending on whether the input IF signal is above or below the ‘ground’ level, respectively. The TTL output from the comparator is sampled in a D-type flip-flop (74LS74) at a rate of 2.04 MHz, which is marginally higher than the required sampling rate (2 MHz corresponding to the IF bandwidth of 1 MHz in the present case, [12]). This means that the 5th harmonic of the sampling clock will fall exactly at the outer edge of the IF band in the present case, i.e. at 11.2 MHz. So we get the entire 1 MHz band without any aliasing problem which otherwise might lead to a reduction in the signal-to-noise ratio [2]. An Ex-OR gate (74LS86) is used to demodulate the sampled signal for Walsh switching [1, 6, 7, 17, 22]. Then it flows through delay lines constructed using a combination of shift registers (74LS164) and multiplexers (74LS151). The necessary delay is implemented under the control of a computer up to a maximum of  $\approx 7.5 \mu\text{s}$  in steps of  $\sim 0.5 \mu\text{s}$ . For the 2.04 MHz sampling rate, the maximum delay error ( $\approx 0.25 \mu\text{s}$ ) causes a coherence loss of about 10% for a 1 MHz bandwidth [18].

The GRH correlator was built using chips primarily designed for the Nobeyama radioheliograph (NRH, [11]). These are custom built double side band (DSB) chips using CMOS gate array technology. Each chip is composed of 4 complex correlator units. There are three 4-bit parallel Ex-OR circuits, one 4-bit parallel Ex-NOR circuit, two addition circuits, two integration circuits, a latch, and a multiplexer circuit in each unit. Figure 1 shows a unit of the correlator chip. It is to be noted that in the 22-bit counter used for integration, the 6 LSB<sup>s</sup> are truncated and only the 16 MSB<sup>s</sup> are read out. The functional diagram of the chip is shown in Figure 2, where  $C^s$  and  $S^s$  are the cosine and sine IF signal corresponding to each antenna. The output of the correlator 1 (cosine correlation) is,

$$C_1 \oplus C_2 + S_1 \oplus S_2 \quad (1)$$

and the output of the correlator 2 (sine correlation) is,

$$C_1 \oplus S_2 + S_1 \oplus C_2 \quad (2)$$

Here  $\oplus$  and  $\oplus$  represent Ex-OR and Ex-NOR operation, respectively. Similarly the other correlators give corresponding outputs. Thus for each antenna pair, the chip gives four correlations compared to two by a single side band (SSB) correlator.

### 3. Amplitude information using a 1-bit correlator

The output of the quantizer (zero-crossing detector) in a 1-bit correlator is either ‘high’ or ‘low’ with no information on the absolute strength of the signal (like in correlator systems with Automatic Gain Control loop) since only the sign of the input waveform is retained. So, the output of the correlator is proportional to the ratio between the correlated power and the sum of the correlated and uncorrelated power. If  $T_s$  is the source brightness temperature and  $T_b$  is the sky background temperature, then the measured correlation coefficient is,

$$\rho_m \propto \frac{T_s}{T_s + T_b} \quad (3)$$

This results in identical correlations for a weak source in a weak background and a strong source in a correspondingly strong background [20]. On the other hand, the output of the

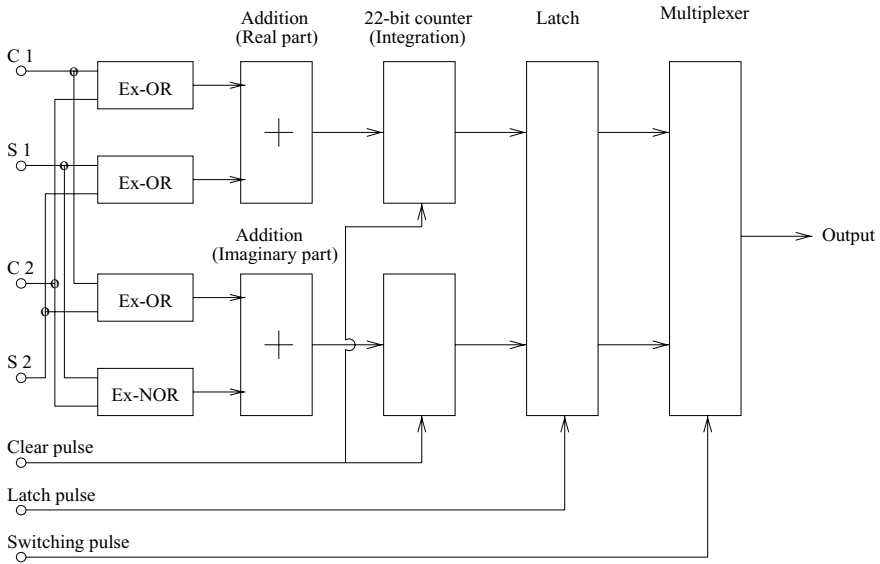
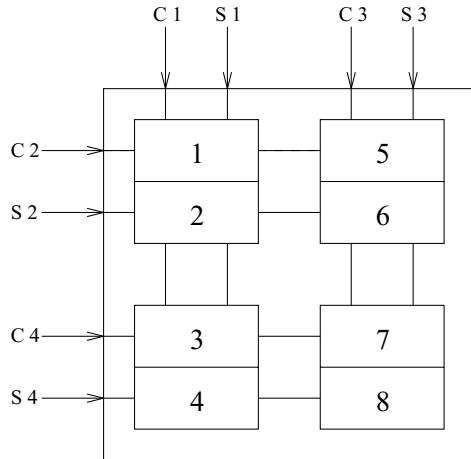


**Fig. 1** An elementary circuit of the correlator chip

**Fig. 2** Functional diagram of the correlator chip



analog correlator is,

$$\rho_r \propto T_s \tag{4}$$

Therefore in order to get the above correlation co-efficient in the case of a 1-bit digital correlator receiver, the total power received by the antenna i.e.  $(T_s + T_b)$  has to be measured separately and multiplied with the measured correlation co-efficient  $(\rho_m)$ . The following scheme originally devised by [19] effectively uses the 1-bit correlator itself to determine the amplitude of the signal (refer [15] for details).

1. Compare the input signal voltage with a known threshold  $V_{th}$ .  
If the amplitude is  $> V_{th}$ , then the comparator output = 1  
Else, the output = 0
2. Sample the output of the comparator.
3. Correlate the sampled signal with 0 and measure  $\rho_m$ .

It can be shown that the measured correlation coefficient,

$$\rho_m = \text{erf} \left( \frac{V_{th}}{\sqrt{2}\sigma} \right) \quad (5)$$

Since  $V_{th}$  is known, the value of  $\sigma$  in Equation (5) can be obtained from the measured values of  $\rho_m$  using standard error function tables [13]. Observationally, the value of  $\rho_m$  is given by,

$$\rho_m = \frac{2N_c}{N} - 1 \quad (6)$$

where  $N_c$  &  $N$  are the number of clock samples and correlations, respectively, in one integration period. Combining this with Van Vleck correction [21], the relation between the correlation co-efficient ( $\rho_t$ ) of the unquantized case (analog correlator) and the observed correlation count  $N_c$  in a 1-bit correlator is,

$$\rho_t = \sigma_1 \sigma_2 \sin \left[ \frac{\pi}{2} \left( \frac{2N_c}{N} - 1 \right) \right] \quad (7)$$

where  $\sigma_1$  and  $\sigma_2$  are the rms values of the input signal voltage to the correlator measured using the aforementioned scheme.

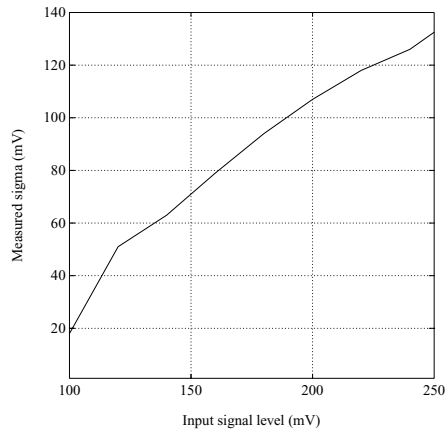
### 3.1. Calibration of the threshold voltage $V_{th}$

A proper selection of the threshold voltage ( $V_{th}$ ) is very crucial getting a correct value for ( $T_s + T_b$ ). In the case of GRH, we estimated the variation in the output of the threshold detector with the input level for different values of  $V_{th}$ . The value of  $\sigma$  was calculated from the measured correlation coefficient  $\rho_m$  for various peak-to-peak values ( $V_{pp}$ ) of the input noise signal. The test was repeated for different values of  $V_{th}$ . It was found that when  $V_{th} \approx 50$  mv, the output was linear with the input for values of  $V_{pp}$  in the range 150–200 mV (Figure 3). To verify our experimental results, we carried out observations of the sky background in the direction of the cosmic radio sources Cassiopeia A and Cygnus A with the above settings. The ratio of the observed sky background temperature, i.e.  $\frac{T_b(CasA)}{T_b(CygnA)}$  was found to be  $\approx 0.66$ . The corresponding value estimated from the literature is  $\approx 0.70$  [10].

## 4. Walsh switching

The coaxial cables that transmit RF signal from different antenna groups in the GRH are well separated. The IF cables and A/D convertors are carefully shielded. In spite of these precautions we found that there is a certain amount of cross-talk between the individual

**Fig. 3** Results of the test for calibration of the threshold detector.



signal channels. Assuming that most of it occurs between the signal flowing through coaxial cables, the RF output from each antenna group is switched by passing it through an electronic switch, controlled by the Walsh function signal transmitted from the receiver building. These switches are kept in the field immediately after the group amplifier. The switching period for each group is different and is a fraction of the time period for which the data is integrated. This implies that the crosstalk signal will get averaged to zero as they will be correlated positively and negatively during either half of the integration period [18]. This switching sequence is subsequently removed at the output of the sampler (using the same Walsh function), thereby also eliminating any errors due to possible DC offsets in the A/D converters. It must be noted that the spurious signal will average to zero through switching only if its amplitude is constant over a Walsh cycle, i.e. it should not be a fringe frequency waveform. Otherwise the cross-coupled signals may not get cancelled exactly. In the case of GRH, the fastest fringe frequency variation is about 21 s, whereas the largest period amongst the 32 Walsh switching functions is  $\approx 251$  ms, i.e. the integration time used in the receiver system. This ensures that the cross-talk signal get averaged to zero.

#### 4.1. DC offset in the A/D convertor

The DC offset occurs in the comparator where the input analog signal gets digitized. We use a 1-bit correlator in the GRH. The ‘zero’ level of the comparator may have an offset, in practice. Because of this, the digitized output from the comparator will be affected and ultimately there will be spurious correlation. The latter will limit the dynamic range of the synthesized image [4]. But the effect of this DC offset can be minimised through the use of Walsh switching. Figures 4 and 5 show the output of one of the cosine correlators in the GRH, without and with Walsh switching, for uncorrelated noise. Note that for a sampling rate of 2.04 MHz and an integration time of  $\approx 251$  ms, the architecture of the correlator chip used in the GRH gives a correlation count of 15356 for full correlation, 7678 for zero correlation and 0 for anti-correlation. An inspection of the above two figures clearly show that when Walsh switching is employed, the average observed count is close to the expected value and also it remains steady (Figure 5).

**Fig. 4** Correlator output for comparator DC offset test WITHOUT Walsh switching

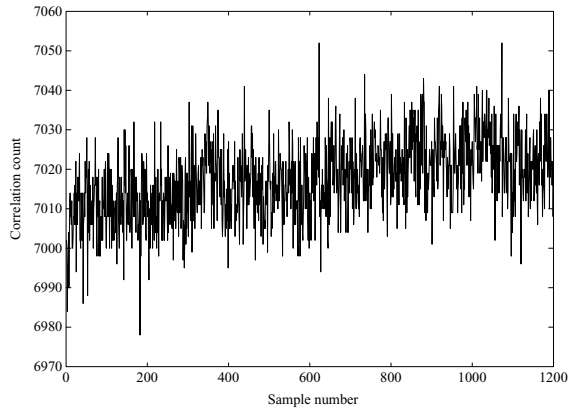
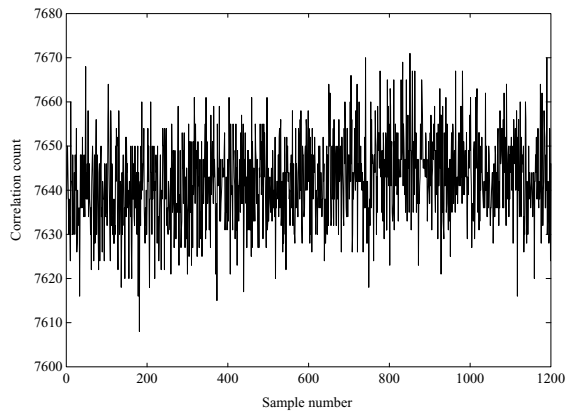


**Fig. 5** Same as Figure 4, but WITH Walsh switching



#### 4.2. Cross-talk between antenna signals

The cross-talk between the different signal paths in a two-element interferometer system will give rise to phase error in the observed complex visibility. It is given by (see [15] for details),

$$\Delta\theta_{mn} = \frac{2\sqrt{\eta}T_{\text{sys}}}{\delta_{mn}T_s} \tag{8}$$

where  $T_{\text{sys}}$  is the system noise,  $\eta$  is the cross-talk factor between the two antennas and  $\delta_{mn}$  is the amplitude of the Fourier component corresponding to the source.  $T_{\text{sys}}$  consists of both the antenna temperature  $T_s$  due to the source and the receiver noise  $T_r$ . One can notice that the phase error varies inversely as the amplitude of the Fourier component corresponding to the source. This implies that the effect of cross-talk will be more particularly on those baselines where the source gets resolved. Figures 6 and 7 show the correlation count obtained by observing the emission from the sky background without and with Walsh switching. Since the emission is mostly uncorrelated, the measured correlation count should be approximately 7678 as mentioned earlier, in the absence of any cross-talk between the signal channels. Figure 6 illustrates how the output is influenced by the cross-talk between the signal channels

**Fig. 6** Correlator output for cross-talk test WITHOUT Walsh switching

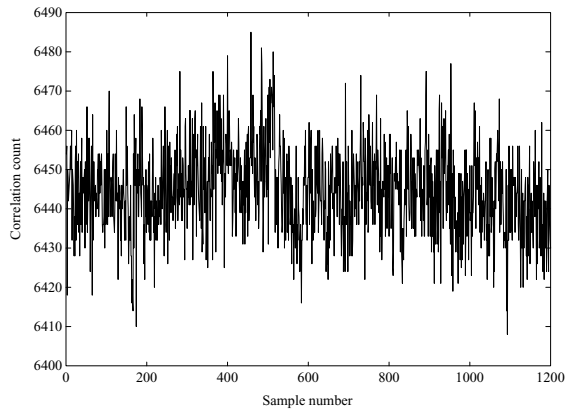
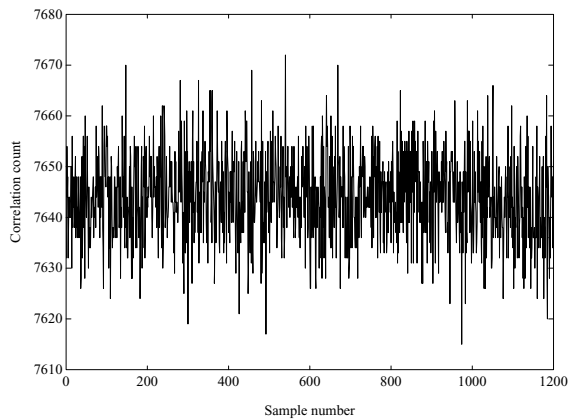


**Fig. 7** Same as Figure 6, but WITH Walsh switching



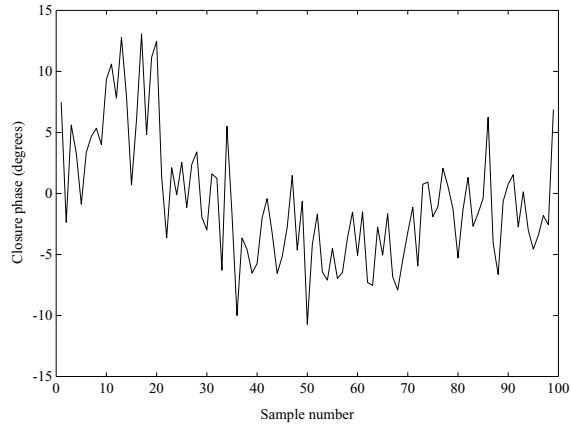
in the absence of Walsh switching. But when Walsh switching is employed, the cross-talk signals get averaged out and the observed count is close to the expected value (Figure 7).

We also verified the effect of switching by estimating the residual phase error in the closed loop of baselines [9] formed by antenna groups 8, 9 and 17 in the GRH and the results are shown in Figure 8. The r.m.s. variation in the error  $\approx 3^\circ$ . Note that we specifically considered the above 3 antenna groups since the u and v-components of baselines formed by these antenna groups are the smallest in the GRH. Therefore any possible non-closing errors due to large scale structures in the sky background should be large in this set (refer [16] for details on the phase calibration scheme used in GRH).

## 5. Testing of the correlator chips

The two major source of errors in any correlator chip are: (1) imperfections in the counters and (2) accuracy of the correlator clock. To check the effect of these errors on the observed correlation count, we carried out a test by leaving the inputs to the correlator ‘open’. This implies that the default input will be TTL ‘high’. As mentioned earlier, the correlator chip used in the GRH uses two correlators for each one of the cosine and sine outputs. Therefore for a fully correlated signal, the number of counts accumulated in the counter for the cosine channel

**Fig. 8** Closure phase obtained on the cosmic radio source Cygnus A (a point source for the GRH) by summing the observed phases on the baselines formed by the multiplications (8, 9), (9, 17) and (8, 17). The successive samples are separated by about 4.64 s



should be  $2 \times 2.04 \times 10^6 \times 251 \times 10^{-3} \approx 1024000$ . These counts get accumulated in a 22-bit counter. Since we read only the 16 MSB<sup>s</sup>, the expected number of counts is,  $1024000/2^6 = 16000$ . The corresponding count in the sine channel should be 8000 (Equations (1) and (2)). The measured correlation counts in the cosine and the sine outputs of the correlator were 15356 and 7678. The difference between the expected and the actual number of counts is due to the effective integration time being less than 251 ms, i.e.,  $(251 \times 10^{-3} - \Delta t)$  s, where  $(\Delta t)$  s, is used for resetting the counters before the start of every new integration period. Though this test is sufficient to check the behaviour of the counter, we performed another test to examine the different stages of the counter. One of the inputs to the correlator was left open as earlier, while a 2.04 MHz square waveform was given at the other input. The cosine output of the correlator for different duty cycles of the input 2.04 MHz square waveform is shown in Figure 9. Since the output increases linearly with the input, it is clear that different stages of the counter are working satisfactorily. The sine output remained constant at 7586, irrespective of the duty cycle of the input 2.04 MHz square waveform. As one can notice from Equation (2), this behaviour is expected since an increase in the duty cycle of the 2.04 MHz waveform increases the correlation corresponding to  $C_1 \oplus S_2$  and decreases the correlation corresponding to  $C_2 \oplus S_1$ . It is to be noted that we have used a 2.04 MHz square waveform, since the correlator clock speed used in the test was also 2.04 MHz. Any imperfections in the correlator clock should be more pronounced in this case.

## 6. Correlator input level vs residual offset

Though Walsh switching scheme is helpful in bringing down the level of the spurious correlation due to DC offset in the comparator and cross-talk between the signal channels, there is always a residual offset present in the output of the correlator, as one can notice from Figures 5 and 7. The mean of the observed correlation count for uncorrelated noise at the input of the correlator is not equal to 7678 as pointed out in Section 5. We carried out a test to understand the effect of this residual on the level of the input signal (correlated) to the correlator. The results (Figure 10) indicate that even if the input signal is fully correlated, the output correlation count (cosine channel) does not show any change until the signal level is  $\geq 200$  mV. So we maintain this as the minimum level of input to the correlator during our regular observations. The correlation count in the sine channel remained approximately

**Fig. 9** Variation of the correlator output (cosine channel) for increasing duty cycle of the input 2.04 MHz square waveform

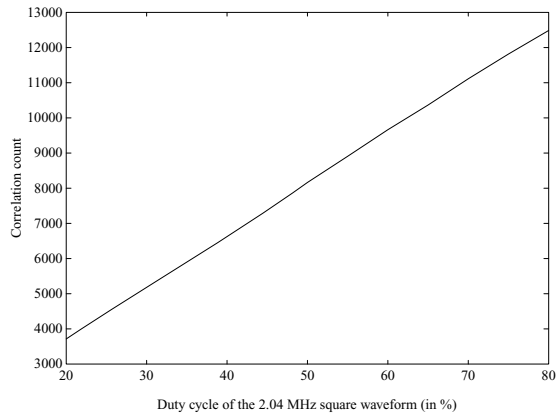
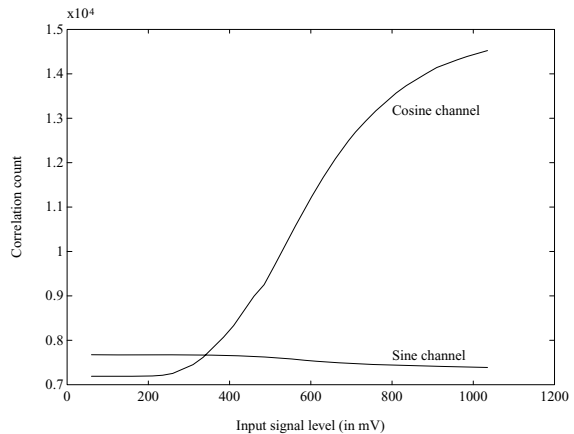


**Fig. 10** Variation of the correlator output for different levels of the input (correlated) signal



constant as expected, for different levels of the input. Even for the maximum level of the input, the phase error due to the variation in the sine channel output was only  $2^\circ$ . It is essential that this phase error is small, since the SNR on different baselines will not be the same while observing extended sources like Sun.

**Acknowledgements** We thank H. Nakajima of the Nobeyama Radio Observatory for his kind assistance in procuring the correlator chips used in the GRH. We had useful discussions with him and M. Nishio of Kagoshima University for the GRH correlator system. N. Udaya Shankar and A.A. Deshpande of Raman Research Institute are thanked for their suggestions in connection with the total power measurement and delay system, respectively. The assembling and testing of PCBs in the GRH correlator system was done by E. Ebenezer and D. Babu. We acknowledge their help. We are grateful to the referee for his useful suggestions in revising the manuscript.

## References

1. Beauchamp, K.G.: Walsh functions and their applications, Academic Press (1975)
2. Brigham, E.O.: The fast Fourier transform and its applications, Prentice Hall (1988)
3. Burns, W.R., Yao, S.S.: Radio Sci. 4(5), 431 (1969)

4. Ekers, R.D.: 1989, in: R.A. Perley, F.R. Schwab, A.H. Bridle (eds.), *Synthesis Imaging in Radio Astronomy*. Astr. Soc. of the Pacific **6**, 1896.
5. Goldstein, R.M.: IRE Trans. Space Electron Telemetry **8**(2), 170 (1962)
6. Granlund, J., Thompson, A.R., Clark, B.G.: IEEE Transactions of Electromagnetic Capability **EMC-20**(3), 451 (1978)
7. Harmuth, H.F.: IEEE Spectrum **6**, 82 (1969)
8. Isbell, D.E.: IRE Trans. Ant. Prop. **AP-8**, 260 (1960)
9. Jennison, R.: MNRAS **118**, 276 (1958)
10. Krauss, J.D.: *Radio Astronomy*, McGraw-Hill (1966)
11. Nakajima, H. et al.: Proc. IEEE **82**(5), 705 (1994)
12. Nyquist, H.: Trans. Am. Inst. Elect. Eng. **47**, 617 (1928)
13. Press, W.H., et al.: *Numerical Recipes in Fortran*, Cambridge University Press (1992)
14. Ramesh, R., et al.: Solar Phys. **181**, 439 (1998a)
15. Ramesh, R.: Ph.D. Thesis, Bangalore University (1998b)
16. Ramesh, R., Subramanian, K.R., Sastry, Ch. V.: Astron. Astrophys. Suppl. **139**, 179 (1999)
17. Thompson, A.R.: VLA Elec. Memo. 122 (1974)
18. Thompson, A.R., Moran, J.M., Swenson Jr., G.W.: *Interferometry and Synthesis in Radio Astronomy*, Wiley-InterScience (1986)
19. Udaya Shankar, N.: Ph.D. Thesis, Bangalore University (1986)
20. Udaya Shankar, N., Ravi Shankar, T.S.: J. Astrophys. Astron. **11**(3), 297 (1990)
21. Van Vleck, J.H., Middleton, D.: Proc. IEEE **54**(1), 2 (1966)
22. Walsh, J.L.: Amer. J. Math. **55**, 5 (1923)
23. Weinreb, S.: Proc. IRE **49**, 1099 (1961)
24. Weinreb, S.: A digital spectral analysis technique and its application to radio astronomy. M.I.T. Res. Lab. of Electronics Tech. Report No. **412** (1963)